

Entropy Analysis in Magnetohydrodynamic Eyring-Powell GO/Blood Nanofluid over an Exponentially Stretching Sheet

Tahir Naseem^{*1,2}, Azeem Shahzad¹, Fateh Mebarek-Oudina²

1. Department of Mathematical Sciences, University of Engineering and Technology, Taxila, 47050, Pakistan.

2. Department of Physics, Faculty of Sciences, University of 20 août 1955-Skikda, B.P 26 Road El-Hadaiek, 21000, Skikda, Algeria

*Corresponding Author **

Abstract

Researchers aim to develop groundbreaking therapies for tissue damage and illness by exploring and enhancing the potential of graphene oxide in various medical domains. Due to its biocompatibility, mechanical properties, electrical conductivity, and ability to interact with biological molecules, graphene oxide shows significant potential for tissue repair and regeneration. This study aims to analyze the entropy of an Eyring-Powell (graphene oxide-blood) nanofluid, distorted by an exponentially stretching sheet. The research examines heat transfer in an Eyring-Powell nanofluid containing five types of nanoparticles: blades, bricks, cylinders, platelets, and spheres. It incorporates effects such as viscous dissipation, radiation, Joule heating, and magnetohydrodynamics.

A set of governing equations is transformed into a dimensionless system using appropriate transformations. Graphs illustrate the physical behavior of temperature and velocity fields. Additionally, the entropy and Bejan number are graphically represented concerning various factors. The skin friction coefficient and Nusselt number are presented graphically. The widely recognized convergence method, BVP4C, is employed to obtain the solution. The comparison of results of the proposed scheme with the existing literature is given in the form of table. Notably, platelet-shaped nanoparticles exhibit the highest entropy among all forms, suggesting that their greater entropy generation implies enhanced heat dissipation capacities. Controlling heat production is essential in medical contexts, such as wound healing or tissue restoration, to prevent tissue damage or necrosis. Platelet-shaped nanoparticles can effectively disperse excessive heat produced during procedures, such as photo-thermal therapy, thereby minimizing potential harm to surrounding tissues.

Keywords: Eyring-Powell Model, Magnetohydrodynamics, Joule Heating, Viscous Dissipation, Radiation, Entropy Analysis.

1. Introduction

Eyring-Powell fluids belong to a specific class of non-Newtonian fluids. They can be categorized into differential types, integral models, and shear rate models. Non-Newtonian fluids play an important role in many engineering, manufacturing, and industrial applications, including processes like boiling, bubble creation, column processing, and plastic foam processing. Hussien [1] investigated the Eyring-Powell nanofluid by considering magnetohydrodynamics over vertical tubes. He found that the Eyring-Powell nanofluid has the capacity to reduce thermal resistance and axial velocity in the vicinity of the walls in diverging channels. Furthermore, his work reveals that the magnetic parameter has a considerable influence on both types of channels. [2] considered the modified Eyring-Powell fluid using Buongiorno's nanofluid correlation model, focusing on the investigation of bioconvection and gyrotactic microorganisms. He also incorporated nonlinear radiation and heat sink sources into the energy equation. He found that when the Biot number and radiation parameter increase, the temperature rises, whereas the Prandtl number exhibits the opposite effect. Additionally, it was observed that as the Lewis number rises, the concentration of gyrotactic microorganisms decreases.

[3] investigated the modified Eyring-Powell model on a linearly stretching flat plate and discovered that temperature decreases with increasing Prandtl number. It was also observed that an increase in the Eyring-Powell parameter leads to a decrease in both the skin friction coefficient and the Nusselt number. Hayyat et al. [4] considered the Eyring-Powell fluid on a moving surface with convective boundary conditions, finding that the thickness of the boundary layer increases with certain parameters and decreases with others. [5] studied the Eyring-Powell fluid that conducts electricity and incorporates Joule heating, radiation, and thermal relaxation time over an exponentially stretching surface. It was found that the thermal relaxation time is inversely proportional to the thickness of the thermal boundary layer and the temperature, while an increase in the Eckert number shows the opposite behavior.

Magnetic fields are referred to as "magneto," fluids as "hydro," and movement as "dynamic." The phrase "magnetohydrodynamics" is a combination of these three terms. Magnetohydrodynamic flow, or MHD flow for short, is the study of the conductive properties of fluids (such as plasmas, liquid metals, saltwater, or electrolytes) under the influence of a magnetic field. For industries developing advanced technologies, it is essential to have a solid understanding of MHD flow. This understanding not only improves industrial processes and contributes to groundbreaking solutions in energy and medicine but also provides essential information about natural phenomena.

[6] investigated the flow, heat, and mass transfer of Eyring-Powell fluid with a microcantilever sensor in a Darcy-Forchheimer porous medium. They analyzed heat and mass transfer, considering the effects of thermal radiation, viscous dissipation, heat generation, activation energy, Soret, and Dufour effects. The authors found that the Hartman number and the fluid coefficient indicate a positive association with the fluid velocity. Conversely, the porosity coefficient, inertia coefficient, and viscosity parameter have a detrimental effect on fluid velocity. Their findings identify thermal radiation, thermal conduction coefficient, Eckert number, heat generation, and Dufour number as potential factors contributing to an increase in temperature within the flow system.

The manipulation of hybrid nanofluids is carried out to precisely regulate the rate of thermal conduction, which is critical for applications in the aerospace and automotive industries, as well as in heating and cooling infrastructure. [7] investigated the Eyring-Powell hybrid nanofluid, which contained both water and nanoparticles, considering the effects of a magnetic field and an unequal heat sink or source. Two different wall jet flow scenarios were analyzed, and numerical solutions were produced for each: one with a magnetic field and one without. The presence of a magnetic field reduces the skin friction value for wall jet flow at the surface by approximately fifty percent, while its absence results in a higher stream function for wall jet flow.

[8] conducted a study on the MHD dissipative Eyring-Powell fluid flow model, which included convective boundary conditions and a magnetic effect on a stretching sheet with slip velocity. Their scientific findings showed that all these parameters increased the nanofluid temperature, except for the slip velocity parameter, which exhibited an opposite trend. Umair and Irfan [9] investigated the effectiveness of Joule heating in a radiative Eyring-Powell nanofluid containing motile gyrotactic microorganisms and Arrhenius activation energy. They found that the presence of Peclet and bio-convective Lewis numbers decreased the number of moving bacteria in the Eyring-Powell fluid. Conversely, higher thermo-Biot and radiation parameters led to an increase in the fluid temperature. Additionally, the concentration field caused an increase in the activation energy parameter. [10] discussed the impact of magnetohydrodynamics (MHD) on the flow of an Eyring-Powell fluid across a permeable and shrinking sheet. They observed that increasing values of magnetic and Eyring-Powell fluid parameters affected the spectrum of feasible solutions. Furthermore, a stability analysis revealed that the first solution remained stable over time, while the second solution displayed instability. For more insight into the Eyring-Powell fluid flow and heat, researchers can refer to papers [11–19] and the references therein.

An irreversible process is one that cannot return to its initial state without consuming energy, even with minuscule changes to the system's properties. Irreversible processes increase the total entropy of the system and its surroundings. Entropy generation quantifies irreversibility in thermodynamic processes, significantly impacting engineering systems.

The study of entropy generation in the context of Eyring-Powell fluid flow across a stretching sheet has practical implications in various industries, such as metallurgy, biomedicine, and coating processes. Understanding the dynamics of irreversibility and its effects on system efficiency is crucial for engineers to improve system effectiveness and energy efficiency.

[20] investigated entropy generation and flow properties using the Eyring-Powell fluid. They found that changes in time scale and viscosity factors led to a decrease in the velocity profile and an increase in the temperature profile. [21] studied the bioconvective flow of Eyring-Powell nanofluid and observed that entropy creation increased with the dispersion of nanoparticles and the density of microorganisms. [22] analyzed the entropy of Eyring-Powell nanofluid flow over a rotating and moving sphere. They considered the coupled convection regime, including the influence of a magnetic field, activation energy, and liquid hydrogen diffusion. The combination of the sphere's angular velocity and the free stream's velocity enabled the observed impulsive motion. In cases of linear combined convection, the development of entropy was shown to be more significant than in cases of nonlinear combined convection. The researchers discovered that a moving sphere could efficiently reduce its entropy production by applying a magnetic field through nonlinear coupled convection. For additional research on the entropy analysis of the Eyring-Powell model over stretching surfaces, see [23-27] and the references therein.

No previous work has investigated the entropy analysis of electrically conductive Eyring-Powell graphene/blood nanofluid with a variety of nanoparticle forms, including blades, bricks, cylinders, platelets, and spheres. This study aims to explore the correlation between radiation, Joule heating, and viscous dissipation on an exponentially stretched sheet. By addressing this gap in the existing literature, the study establishes a framework for future research and provides a platform for academics to extend and improve upon the current body of knowledge.

The paper is organized as follows: the first section presents an exhaustive review of previous works related to the topic. The second section provides a comprehensive explanation of the mathematical framework and equations governing the problem. Section 3 details the approach and numerical techniques used to solve the equations. The presentation and discussion of the results, including graphical and tabular

representations of the data, are covered in Section 4. The fifth section summarizes the key findings and potential avenues for future research.

This structured framework ensures a thorough evaluation of the subject matter and provides clarity regarding the approach and findings, facilitating further academic contributions to the field.

2. The Problem's Formulation

The MHD Eyring-Powell graphene/blood nanofluid flows continuously and smoothly over a stretching sheet. The temperature profile also accounts for the effects of Joule heating, thermal radiation, and viscous dissipation. Figure 1 depicts the suspension of graphene oxide nanoparticles of various shapes—blade, brick, cylinder, platelet, and sphere—in a base fluid, which is blood. The surface is aligned with the x – and y –axes, and the flow is limited to $y \geq 0$. Consider the functions $U_\infty = be^{\frac{x}{l}}$ and $U_w(x) = ae^{\frac{x}{l}}$ which represent the sheet velocity and external fluid velocity, respectively. In addition, the wall temperature is presented by equation $T_w(x) = T_\infty + ce^{\frac{x}{2l}}$, here the ambient temperature is denoted by T_∞ .

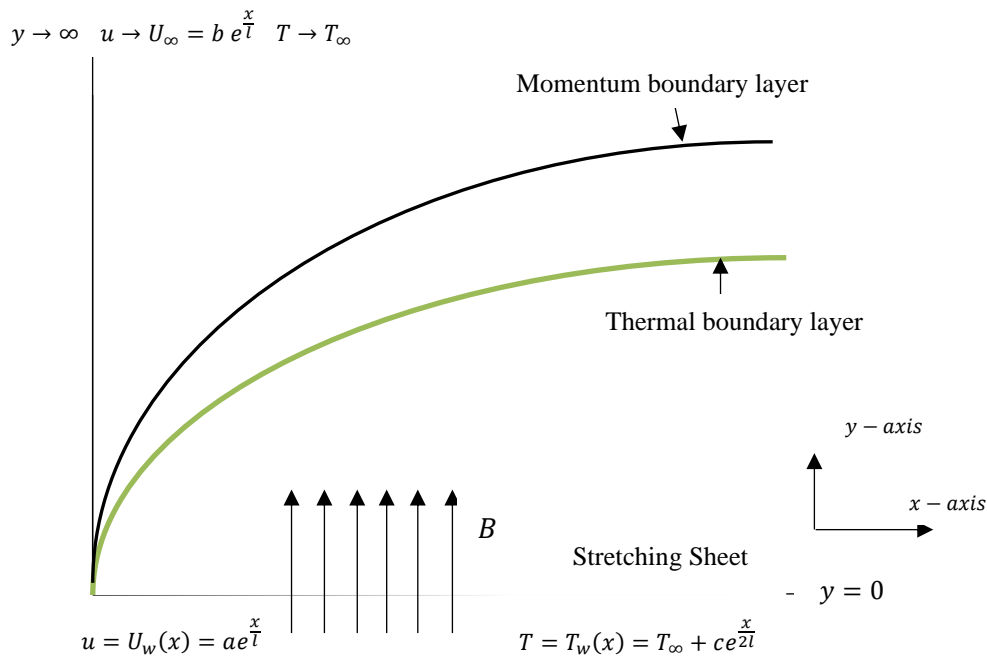


Fig. 1. The schematic diagram of the problem.

The governing equations so obtained are given as [28]

$$\frac{\partial u}{\partial x} + \frac{\partial v}{\partial y} = 0, \quad (1)$$

$$\rho_{nf} \left(u \frac{\partial u}{\partial x} + v \frac{\partial u}{\partial y} \right) = U_{\infty} \frac{dU_{\infty}}{dx} + \left(\mu_{nf} + \frac{1}{\beta C_1} \right) \frac{\partial^2 u}{\partial y^2} - \frac{1}{2\beta C_1^3} \left(\frac{\partial u}{\partial y} \right)^2 \frac{\partial^2 u}{\partial y^2} \quad (2)$$

$$-\sigma_{nf} B_0^2 (u - U_{\infty}),$$

$$(\rho C_p)_{nf} \left(u \frac{\partial T}{\partial x} + v \frac{\partial T}{\partial y} \right) = k_{nf} \frac{\partial^2 T}{\partial y^2} + \left(\mu_{nf} + \frac{1}{\beta C_1} \right) \left(\frac{\partial u}{\partial y} \right)^2 - \frac{1}{6\beta C_1^3} \left(\frac{\partial u}{\partial y} \right)^4 \quad (3)$$

$$+\sigma_{nf} B_0^2 (u - U_{\infty})^2 - \frac{\partial q_{rad}}{\partial y},$$

where

$$\frac{\rho_{nf}}{\rho_f} = (1 - \phi) + \phi \frac{\rho_s}{\rho_f}, \frac{\mu_{nf}}{\mu_f} = (1 + A_1 \phi + A_2 \phi^2), \alpha_{nf} = \frac{k_{nf}}{(\rho C_p)_{nf}}$$

The ratio of thermal conductivity is given by:

$$k_{nf} = k_f \left[\frac{k_s + (m - 1)k_f + (m - 1)(k_s - k_f)\phi}{k_s + (m - 1)k_f - (k_s - k_f)\phi} \right].$$

Here the stream velocity is denoted by U_{∞} , v and u represent component velocity along x and y directions respectively, U_w shows the stretching velocity, T_w and T_{∞} are the fluid surface and ambient temperatures respectively, β and C_1 represent the material factors, and $(\rho C_p)_{nf}$, is the electrical thermal conductivity of the nanofluid, and σ_{nf} is the specific heat. Furthermore, the heat flux due to radiation q_r in the Rosseland approximation is given by:

$$q_{rad} = -\frac{4\sigma^*}{3k^*} \frac{\partial T^4}{\partial y},$$

This equation shows that the radiative heat flux is proportional to the negative gradient of the fourth power of the temperature, indicating a diffusive transport of radiation energy and σ^* is the Stefan-Boltzmann constant, and T is the temperature. By expanding T^4 in a Taylor's series around T_{∞} and neglecting 2nd and higher order terms, we get

$$T^4 = 4T_{\infty}^3 T - 3T_{\infty}^4.$$

The nanoparticle shapes and viscosity enhancement coefficients are shown in Table 1. Table 2 provides the thermophysical properties of base fluids and the nanoparticles.

Table.1. Nanoparticle Shapes and Factors Enhancing Viscosity [29].






Nanoparticle Shapes		Shape factors (m)	A_1	A_2
Blade		8.26	14.6	123.3
Brick		3.72	1.9	471.4
Cylinder		4.82	13.5	904.4
Platelets		5.72	37.1	612.6
Sphere		3.0	2.5	6.5

Table 2. Thermophysical characteristics of nanoparticle and the base fluid.

Physical Properties	Nanoparticle (GO)	Base fluid (Blood)
$\sigma(\Omega^{-1}.m^{-1})$	4.57	0.18
$Cp(J.kg^{-1}.K^{-1})$	717	3594
$\rho(kg.m^{-3})$	1800	1053
$k(W.m^{-1}.K^{-1})$	5000	0.492

The appropriate boundary conditions are

$$\left. \begin{aligned} u = U_w(x) = ae^{\frac{x}{l}}, \quad v = 0, \\ T = T_w(x) = T_\infty + ce^{\frac{x}{2l}}, \quad \text{at } y = 0, \\ u \rightarrow U_\infty(x) = be^{\frac{x}{l}}, T \rightarrow T_\infty, \quad \text{as } y \rightarrow \infty. \end{aligned} \right\} \quad (4)$$

Let us consider the following suitable similarity transformation to convert equations governing equations into ordinary differential equations

$$\eta = \sqrt{\frac{a}{2\nu L}} e^{x/2L} y, u = a e^{\frac{x}{L}} f'(\eta), v = -\sqrt{\frac{\nu a}{2L}} e^{\frac{x}{2L}} [f(\eta) + \eta f'(\eta)], \theta(\eta) = \frac{T - T_\infty}{T_w - T_\infty}. \quad (5)$$

By applying the aforementioned transformation, Equations (2-4) are transformed into the following format, whereas the continuity equation given in equation (1) is identically satisfied.

$$\epsilon_1 \left(1 + \frac{K}{\epsilon_4}\right) f'''' + f f'' - 2f'^2 - \frac{K\Gamma}{\epsilon_5} f''^2 f'''' + 2\lambda^2 - M\epsilon_3(\lambda - f') = 0, \quad (6)$$

$$\left(\frac{\epsilon_2}{Pr} + \frac{Rd}{\epsilon_5}\right) \theta'' + f\theta' - \theta f' + Ec \left(\epsilon_1 + \frac{K}{\epsilon_5}\right) f''^2 - \frac{1}{3} Ec \frac{K\Gamma}{\epsilon_5} f''^4 + MEc\epsilon_3(\lambda - f')^2, \quad (7)$$

$$f(0) = 0, f'(0) = 1, \theta(0) = 1, f'(\infty) \rightarrow \lambda, \theta(\infty) \rightarrow 0, \quad (8)$$

where

$$\lambda = \frac{b}{a}, K = \frac{1}{\mu_f \beta C}, \Gamma = \frac{U_w^3}{4\nu_f L C^2}, Pr = \frac{\mu_f (C_p)_f}{k}, M = \frac{\delta_f}{\rho_f} \left(\frac{2LB_0^2}{U_w}\right), Rd = \frac{16T_\infty^3 \sigma^*}{3k^* (C_p \mu)_f},$$

$$Ec = \frac{U_w^2}{(C_p)_f c e^{2L}}, \epsilon_4 = (1 + A_1 \phi + A_2 \phi^2), \epsilon_5 = (1 - \phi) + \phi \frac{\rho_s}{\rho_f}, \epsilon_1$$

$$= \frac{1 + A_1 \phi + A_2 \phi^2}{1 - \phi + \phi \frac{\rho_s}{\rho_f}}, \epsilon_2 = \frac{\left(\frac{k_{nf}}{k_f}\right)}{1 - \phi + \phi \frac{(\rho C_p)_s}{(\rho C_p)_f}}, \epsilon_3 = \frac{1 - \phi + \phi \frac{\sigma_s}{\sigma_f}}{1 - \phi + \phi \frac{\rho_s}{\rho_f}}. \quad (9)$$

Here, λ present the velocity ratio parameter, Pr the Prandtl number, and K and Γ are the dimensionless fluid parameters. When $K = 0$, the fluid behaves as a Newtonian fluid. The skin friction coefficient C_f and the local Nusselt number Nu are mathematically written as

$$C_f = \frac{\tau_w}{\rho_{nf} U_w^2}, Nu = (1 + Rd) \frac{x q_w}{k_f (T_w - T_\infty)}, \quad (10)$$

Here, τ_w represents the wall shear stress, which is the tangential stress on the wall exerted by the fluid and q_w denotes the heat flux at the wall, which is the rate of heat transfer per unit area at the wall surface. These quantities are mathematically described as

$$\tau_w = \left(\mu_{nf} + \frac{1}{\beta C} \right) \Big|_{y=0} - \frac{1}{6\beta C^3} \left(\frac{\partial u}{\partial y} \right)^3 \Big|_{y=0}, q_w = -k_{nf} \left(\frac{\partial T}{\partial y} \right) \Big|_{y=0}. \quad (11)$$

After applying the selected transformation skin friction coefficient and local Nusselt number takes the form

$$\sqrt{2Re_L} \cdot C_f = \left(1 + \frac{K}{\epsilon_4} \right) f''(0) - \frac{K\Gamma}{3} \cdot (f''(0))^3, \sqrt{\frac{2L}{x}} Nu Re_x^{-\frac{1}{2}} = -\frac{k_{nf}}{k_f} (1 + Rd) \theta'(0), \quad (12)$$

here $Re_L = \frac{U_w L}{\nu}$, and $Re_x = \frac{U_w x}{\nu}$, are local Reynolds numbers.

2.1. Mathematical formulation of Entropy

General form of equation for entropy generation of Powell-Eyring fluid is as follows

$$S_g''' = \frac{-(1 + Rd)}{T_0^2} (q \cdot \nabla T) - \frac{1}{T_0} \tau : \nabla V + \frac{1}{T_0} \left(\frac{1}{\sigma} (J \cdot J) \right), \quad (13)$$

where $q = -k\nabla T$.

Therefore, after using boundary layer approximations and similarity transformation, equation (13) takes the form

$$N_G = \frac{k_{nf} Re_L}{k_f} \frac{1}{2} \left(1 + \frac{4}{3} Rd \right) (\theta')^2 + \frac{Re_L Br}{2\Omega} \left\{ \left(\frac{\mu_{nf}}{\mu_f} \left(1 + \frac{K}{\epsilon_4} \right) \right) (f'')^2 - \frac{\mu_{nf} B K}{\mu_f} \frac{1}{6} (f'')^4 \right\} \\ + \left(1 - \phi + \phi \frac{\sigma_s}{\sigma_f} \right) M (\lambda - f')^2, \quad (14)$$

where

$$N_G = \frac{S_{gen}'''}{S_0'''} \left(= \frac{k_f (\Delta T)^2}{L^2 T_\infty^2} \right), Re_L = \frac{U_w L}{\nu_f}, Br = \frac{\mu_f U_w^2}{k_f \Delta T}, \Omega = \frac{\Delta T}{T_\infty}, K = \frac{1}{\mu_f \beta C}, B = \frac{U_w^3}{2\nu_f L C^2},$$

are the entropy generation, Reynold's number, Brinkman number, dimensionless temperature difference and fluid parameter. In the above equation, the entropy generation consist of three effects: thermal irreversibility, fluid friction irreversibility and the joule heating irreversibility.

3. Solution Methodology

[30] employed BVP4C and the homotopy analysis method to solve the Eyring-Powell fluid flow problem.[31] applied a shooting technique to achieve their goals, while [32] effectively addressed the Eyring-Powell fluid model using a highly precise fourth-order approach. BVP4C is a technique used to solve nonlinear coupled ordinary differential equations. Compared to other numerical and analytical approaches, this technique is more powerful and precise in solving any type of boundary value problem. Figure 2 shows the flowchart of the proposed scheme, which explains the procedure by which BVP4C works.

This technique has various advantages over other methods; for example, BVP4C solves nonlinear ordinary differential equations with exceptional precision. It is highly efficient for handling complex problems with multiple boundary conditions. Furthermore, this method ensures numerical stability even in the case of differential equations with varying coefficients or singularities. Software packages like MATLAB's built-in solver extensively employ BVP4C, ensuring its accessibility for researchers and practitioners across various domains. In general, the BVP4C method is highly accurate in producing precise results, streamlined in performance, resilient, and widely used in tackling intricate boundary value problems related to ordinary differential equation.

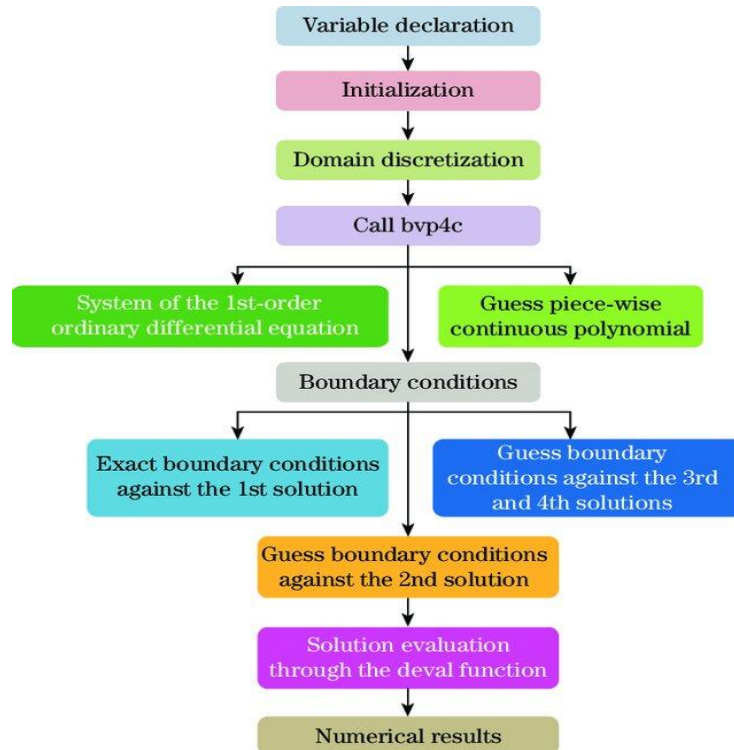


Figure 2. Flowchart of the proposed numerical scheme.

Therefore, the nonlinear ordinary differential equations of the third order (6), as well as the second order (7) and (8), are written as difference equations and solved with the help of the proposed technique by using MATLAB software.

$$f = y_1, f' = y_2, f'' = y_3, f''' = yy1,$$

$$yy1 = \frac{-2M\epsilon_3(\lambda - y_2) - y_1y_3 + 2y_2^2 - 2\lambda^2}{\epsilon_1 \left(1 + \frac{K}{\epsilon_4}\right) - \frac{\Gamma K}{\epsilon_5} y_3^2}, \quad (16)$$

$$\theta = y_4, \theta' = y_5, \theta'' = yy2,$$

$$yy2 = \frac{y_2y_4 - y_1y_5 - MEc\epsilon_3(\lambda - y_2)^2 - Ec \left(\epsilon_1 + \frac{K}{\epsilon_5}\right) y_3^2 + \frac{Ec\Gamma K}{3\epsilon_5} y_3^2}{\frac{\epsilon_2}{Pr} + \frac{Rd}{\epsilon_5}}, \quad (17)$$

$$y_1(0) = 0, y_2(0) = 1, y_5(0) = 1, \quad (18)$$

$$y_2(\infty) = \lambda, y_5(\infty) = 0,$$

The necessary level of accuracy will be achieved through the iterative process.

4. Result and Discussion

This section discusses the effects of nanoparticle shape factors (blade, brick, cylinder, platelets, and sphere) on velocity, temperature, entropy generation number, and Bejan number. Furthermore, by considering pertinent parameters in the entropy equation, these effects are presented graphically. Tables explain terms like the Nusselt number and skin friction, and present comparisons with the existing literature.

Two varieties of boundary layers have developed in close proximity to the sheet in a flow characterized by an exponentially stretching sheet and an ever-changing free stream velocity. This indicates that they are influenced by the velocity ratio parameter $\lambda = b/a$. It is noteworthy to mention that in the case of $\lambda = 1$, the absence of a velocity boundary layer in the vicinity of the sheet is attributed to the fact that both the fluid and the wall are moving at the same speed. The velocity profiles representing different values of λ are illustrated in figure 3. The figure illustrates that the velocity is greater at the wall's surface for values of $\lambda < 1$, whereas it is greater away from the wall for values of $\lambda > 1$. The velocity of platelet nanoparticles in nanofluid is found to be greater, while the velocity of sphere-shaped nanoparticles is

found to be lower. figure 4 illustrates the influence of distinct nanoparticle shapes on the temperature field. The finding that platelet-shaped nanoparticles result in a higher nanofluid temperature compared to sphere-shaped nanoparticles has important practical implications, especially in tissue regeneration. The higher temperature associated with platelet nanoparticles can enhance the thermal effects necessary for accelerating cellular activities and tissue repair processes, making them more effective in regenerative medicine. In contrast, sphere-shaped nanoparticles, which lead to a lower temperature, may be better suited for applications requiring minimal thermal impact, such as maintaining the viability of sensitive tissues during treatment. Understanding these temperature effects allows for the tailored use of nanofluids to optimize therapeutic outcomes in various biomedical applications.

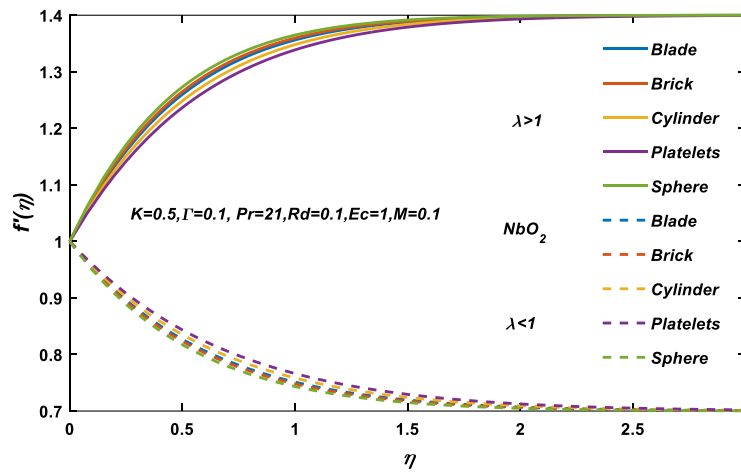


Fig. 3. velocity profile against different shape factors for various values of λ .

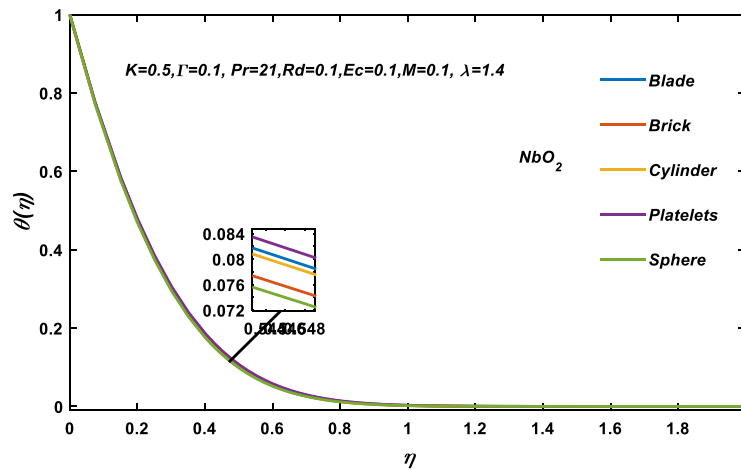
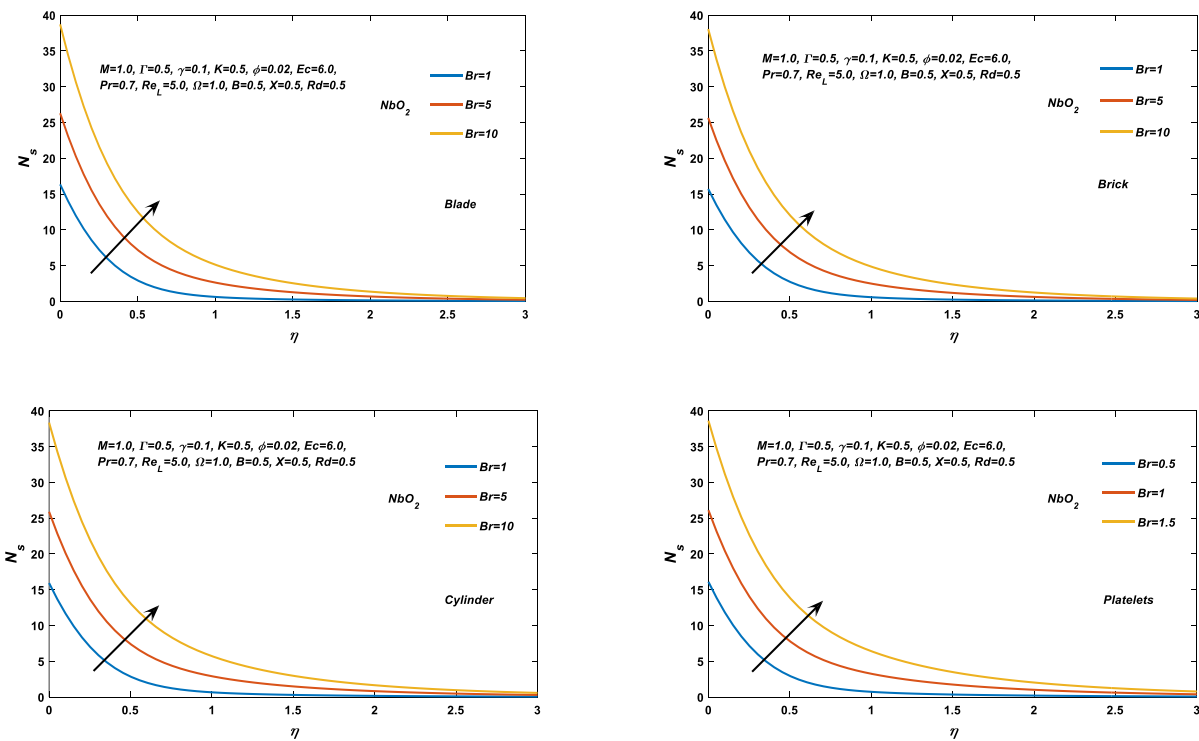


Fig. 4. temperature profile against different shapes factors.

The study of entropy generation in the flow of nanofluids gives us a lot of information about the thermodynamic properties of these fluids and helps us come up with better ways to manage heat that work better and more efficiently. The impact of the Brinkman number on the entropy generation is exhibited in figure 5. It is observed that when the Brinkman number goes up, it means that the flow is facing more resistance because nanoparticles are arranged in different shapes, such as blade, brick, cylinder, and sphere. Elevated levels of flow resistance result in increased irreversible energy dissipation, which in turn contributes to greater entropy.



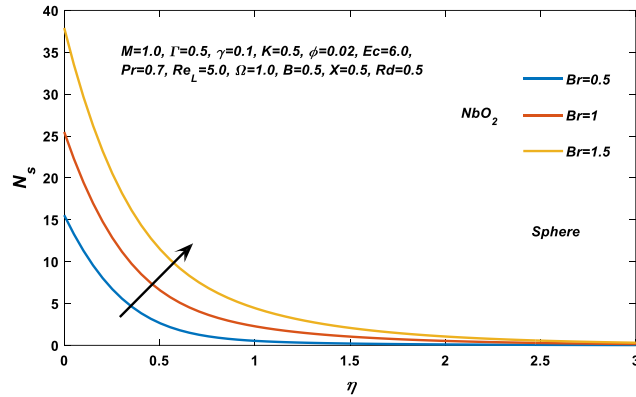
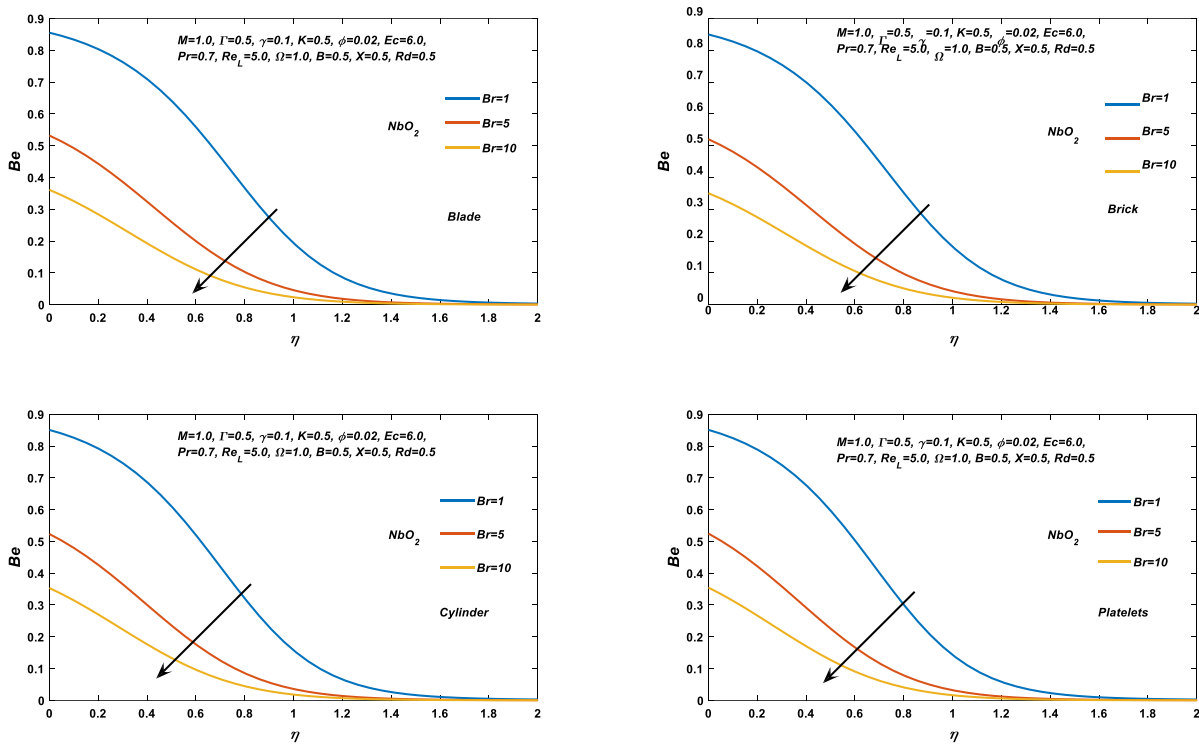


Figure. 5(a – e). Entropy generation for various values of Br.

There is a clear relationship between the increase in the Brinkman number and the rate of heat transfer across the fluid, as opposed to the rate of heat conduction within the fluid. As the Brinkman number increases, heat transmission near the stretching surface may increase. Consequently, the irreversibility of heat transfer gains relative significance. As illustrated in figure 6, since the Bejan number serves as a metric for this relative importance, it tends to decrease in magnitude for the growing Brinkman number.



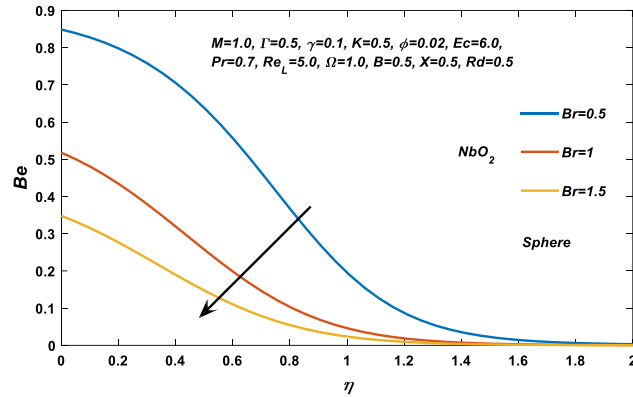
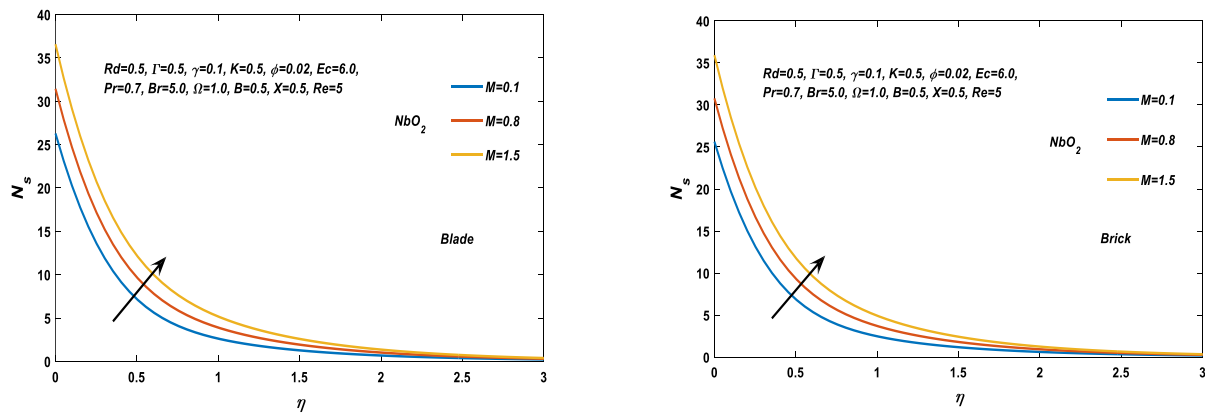


Figure. 6(a – e). Bejan number for various values of Br.

Figure 7 illustrates the influence of magnetic parameters on entropy generation. As the values of magnetic parameters increase, the entropy generation, a measure of the number of irreversible processes in the flow, also increases. This is because the magnetic fields in the MHD flow contribute to the presence of additional sources of irreversibility. Figure 8 illustrates this reverse behavior. The Eyring-Powell model's finding that the Bejan number decreases with increasing magnetic parameters in the flow of graphene/blood nanofluid over an exponential stretching sheet has practical implications for tissue regeneration. The reduction in Bejan number indicates improved heat transfer efficiency and stabilized fluid flow, which are crucial for maintaining optimal temperatures and reducing thermal and flow-related irreversibilities. In tissue regeneration, these effects can enhance the uniform distribution of heat and nutrients, promoting faster and more efficient healing. Additionally, the stabilized fluid flow helps maintain a controlled environment, essential for the delicate processes involved in tissue growth and repair. These insights guide the use of nanofluids to optimize conditions for regenerative medicine applications.



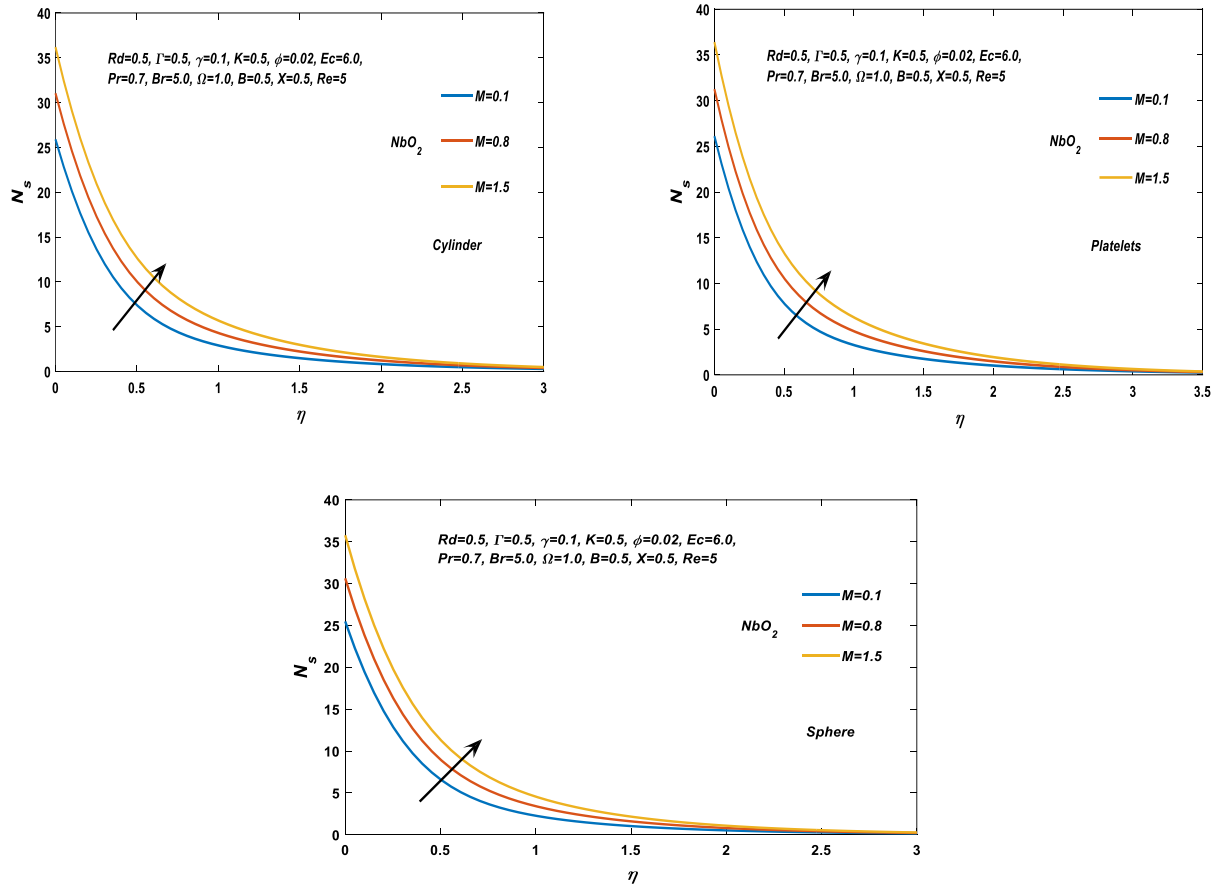
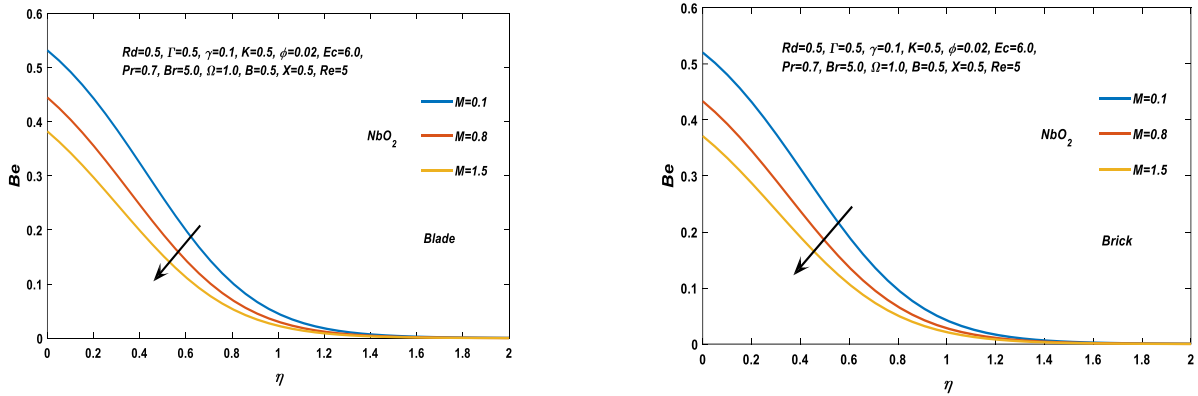


Figure. 7(a – e). Entropy generation for various values of M.



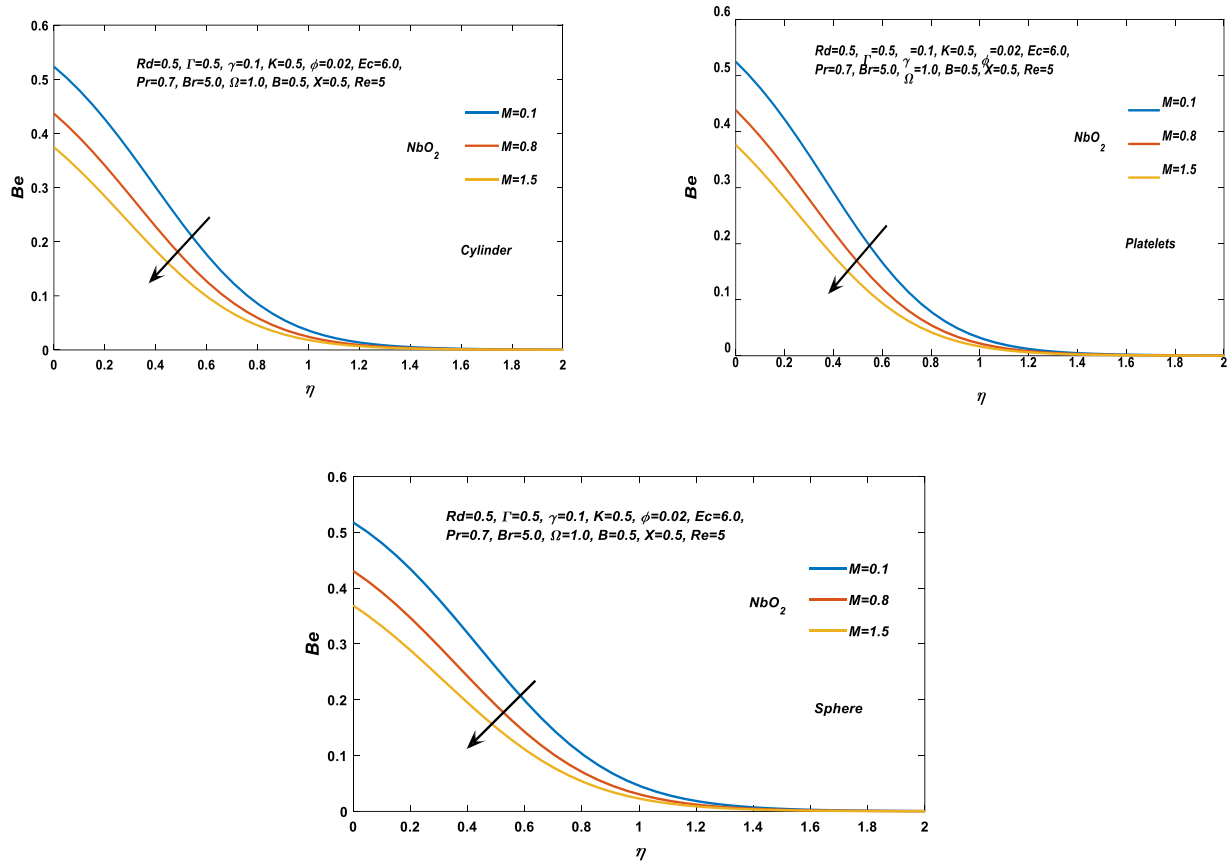


Figure. 8(a – e). Bejan number for various values of M.

The higher entropy production of platelet-shaped nanoparticles in graphene oxide/blood nanofluid, due to their larger surface area and ability to create turbulence and enhance heat transfer, has important implications for practical applications like tissue regeneration. The increased entropy production can improve the efficiency of heat distribution and nutrient transport, crucial for supporting cell growth and repair in tissue engineering. Conversely, the lower entropy production of spherical nanoparticles, resulting in more stable and predictable flow, can be advantageous in applications requiring controlled environments. These findings guide the selection of nanoparticle shapes to optimize performance in various biomedical applications, such as improving the effectiveness of nanofluids in tissue regeneration. This fact is depicted in a clear and transparent manner in figure 9.

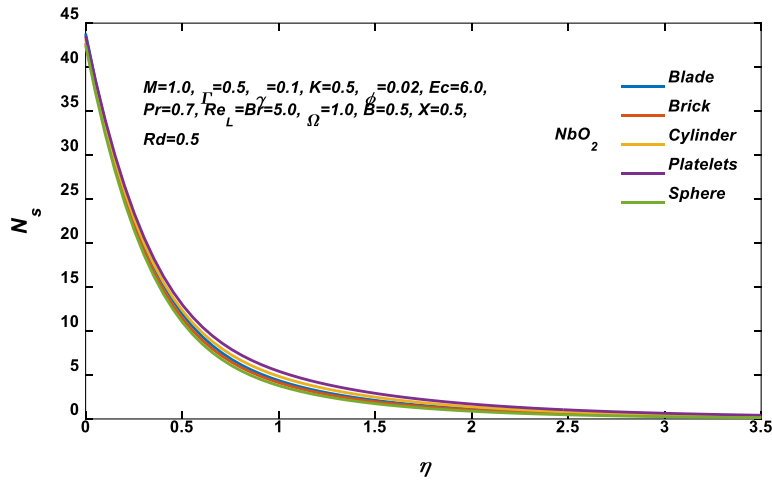


Figure. 9. Entropy generation for various shapes of nanoparticles.

Platelet-shaped nanoparticles often possess a greater surface area compared to spherical nanoparticles, hence augmenting their capacity to conduct heat to the surrounding fluid. The enhanced heat transfer efficiency could potentially lead to a more effective dissipation of temperature differences within the flow, thereby reducing the creation of entropy due to heat transfer inefficiencies and consequently lowering the Bejan number. Spherical nanoparticles, although they retain the ability to improve heat transmission, may not achieve the same level of effectiveness due to their reduced surface area. This can lead to a decrease in heat dissipation efficiency and an increase in entropy formation, resulting in a larger Bejan number. These consequences are illustrated in figure 10.

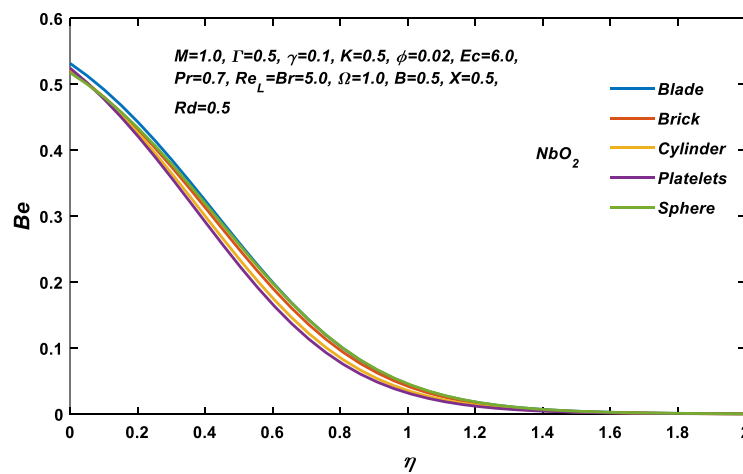


Figure. 10. Bejan number against different shape factors of nanoparticles.

The Nusselt number and skin friction values for the local region can be found in Table 3. The values were determined using a MATLAB algorithm called BVP4C. As K increases, the skin friction coefficient also increases. As Γ increases, the coefficient of friction on the skin decreases. In a study conducted by [5], it was observed that the skin friction coefficient experiences a significant decrease as the velocity ratio increases on an exponentially stretched surface. It has been noted that as K increases, the thickness of the thermal boundary layer decreases. As a result, the rate of heat transfer to the stretched sheet is increased. In addition, when Γ increases, there is a noticeable decrease in the magnitude of the local Nusselt population. In addition, it increases as K and λ values increase.

Table 3. The skin friction coefficient and local Nusselt number changing values of K , λ , and Γ .

K	Γ	λ	$-f''(0)$			$-\theta'(0)$		
			HAM [28]	Present	BVP4C [5]	HAM [28]	Present	BVP4C [5]
0.0	0.1	0.1	1.253580	1.2535801	1.2535773	0.977953	0.76176461	1.8186356
0.5			1.530419	1.520614	1.5206131	1.022158	1.8237173	1.8950494
1.0			1.766459	1.766456	1.7537186	1.050549	1.835459	1.9418477
1.5			1.975250	1.9615858	1.9895533	1.070644	1.8397829	1.9737646
0.5	0.0		1.535315	1.5353157	1.535315	1.023016	1.8222476	1.894993
	0.5		1.509342	1.4599116	1.4599118	1.018406	1.8297362	1.8952861
	1.0		1.478121	1.3793083	1.3793085	1.012648	1.8376014	1.8955991
	1.5		1.414220	1.2925794	1.2925796	1.003943	1.8458935	1.8959392
	0.5	0.2	1.441522	1.3986012	1.3986012	1.040756	1.9012664	1.9507173
		0.3	1.343664	1.3091033	1.3091033	1.066060	1.9870086	2.0135636
		0.5	1.069109	1.0519635	1.0519635	1.119838	2.1731917	2.146434
		0.7	0.701535	0.69676492	0.69676493	1.174081	2.3492452	2.2765247

5. Concluding Remarks

An investigation is conducted on the entropy of the Eyring-Powell model NbO_2 /blood nanofluid over a sheet that is being exponentially stretched. The study examined how different shape parameters of GO nanoparticles affect the velocity and temperature profile of Eyring-Powell Graphene Oxide/blood nanofluid. In addition, the study examined the impact of the Brinkman number (Br), magnetic parameter

(M), and form factor of nanoparticles on entropy generation and Bejan number. Below are the key characteristics of the study.

- The platelets shape nanoparticles of Graphene oxide in Eyring-Powell GO/blood nanofluid had highest velocity whereas the sphere shape nanoparticles had the lowest one for the stretching parameter less than one while the reverse effect was observed for stretching parameter greater than one.
- The maximum and minimum temperature profile was observed for platelets shape and sphere shape nanoparticles, respectively.
- It is observed that the irreversibility of heat transfer, resulting from limiting temperature differences, and the irreversibility of fluid friction, both contribute to a rise in the total entropy generation, even while the Bejan number decreases. As for the increased in Brinkman number, the formation of entropy due to fluid friction and Joule dissipation also increased. However, the Bejan number showed the opposite tendency. The similar trend is observed in the case of magnetic parameter.
- The spherical nanoparticles had the lowest level of entropy generation, whereas the platelet-shaped nanoparticles revealed the highest level. The Bejan number exhibits inverse behaviour.

Moreover, the increased entropy generation seen in platelet-shaped nanoparticles may suggest enhanced fluid dynamics. In medical contexts involving fluid dynamics, such as drug administration or tissue engineering, the capacity of nanoparticles to impact flow patterns can be advantageous. Platelet-shaped nanoparticles have the potential to enhance medication dispersion or cell seeding in tissue scaffolds, hence improving therapeutic effects. The study's findings are confirmed by the utilization of simulations to assess the skin friction coefficient and local Nusselt number.

6. Nomenclature

U_w	Stretching velocity, m/s	λ	Ratio of expansion rates
u, v, w	Velocity components, m/s	K, Γ	Dimensionless Eyring – Powell fluid parameters
U_∞	Velocity of external flow, m/s	Pr	Prandtl number
L	Characteristic length, m	C_f	Skin friction coefficient

T_w	Surface temperature, K	Nu	Local Nusselt number
T_∞	Ambient temperature, K	τ_w	Wall shear stress
τ	Stress tensor, N/m^2	q_w	Surface heat flux
ν	Kinematic viscosity, m^2/s	Re, Re_x	Local Reynolds numbers
μ	Dynamic viscosity, $Kg/m.s$	B	Magnitude of magnetic field
ρ	Density of the fluid, Kg/m^3	q_{rad}	Radiative heat flux
β	Eyring – Powell material parameter, $(Pa)^{-1}$	K^*	Mean absorption coefficient, m^{-1}
C	Eyring – Powell material parameter, s^{-1}	σ^*	Stefan Boltzmann constant, $W/m^2.K^4$
C_p	Specific heat, $J/Kg.K$	k	Thermal conductivity of the fluid , $W/m.K$
T	Temperature of the fluid, K		
$\epsilon_1, \epsilon_2, \epsilon_3$	Constants	Ec	Eckert number
Rd	Radiation parameter	M	Magnetic parameter

Funding Statement: This study has received no funding.

Data access statement: The paper and its supporting materials contain all pertinent information.

Conflict of Interest Statement: The authors affirm that they have no financial stake in the subject matter or the contents covered in this book and that they are not associated with or involved with any group or company that does.

References

- [1] Hussein, S.A., 2023. Simulating and interpretation of MHD peristaltic transport of dissipated Eyring–Powell nanofluid flow through vertical divergent/nondivergent channel. *Numerical Heat Transfer, Part A: Applications*, 84(10), pp.1124-1148.

- [2] Khan, W.A., 2023. Dynamics of gyrotactic microorganisms for modified Eyring Powell nanofluid flow with bioconvection and nonlinear radiation aspects. *Waves in Random and Complex Media*, pp.1-11.
- [3] Oke, A.S., 2022. Theoretical analysis of modified Eyring Powell fluid flow. *Journal of the Taiwan Institute of Chemical Engineers*, 132, p.104152.
- [4] Hayat, T., Iqbal, Z., Qasim, M. and Obaidat, S., 2012. Steady flow of an Eyring Powell fluid over a moving surface with convective boundary conditions. *International Journal of Heat and Mass Transfer*, 55(7-8), pp.1817-1822.
- [5] Naseem, T., Bibi, I., Shahzad, A. and Munir, M., 2023. Analysis of heat transport in a Powell–Eyring fluid with radiation and joule heating effects via a similarity transformation. *Fluid Dynamics & Materials Processing*, 19(3), pp.663-677.
- [6] Awais, M., Salahuddin, T. and Muhammad, S., 2024. Effects of viscous dissipation and activation energy for the MHD Eyring-powell fluid flow with Darcy-Forchheimer and variable fluid properties. *Ain Shams Engineering Journal*, 15(2), p.102422.
- [7] Yaseen, M., Rawat, S.K., Khan, U., Sarris, I.E., Khan, H., Negi, A.S., Khan, A., Sherif, E.S.M., Hassan, A.M. and Zaib, A., 2023. Numerical analysis of magnetohydrodynamics in an Eyring–Powell hybrid nanofluid flow on wall jet heat and mass transfer. *Nanotechnology*, 34(48), p.485405.
- [8] Abbas, W., Megahed, A.M., Emam, M.S. and Sadek, H.M., 2023. MHD dissipative Powell-Eyring fluid flow due to a stretching sheet with convective boundary conditions and slip velocity. *Scientific Reports*, 13(1), p.15674.
- [9] Ali, U. and Irfan, M., 2024. Thermal performance of Joule heating in radiative Eyring-Powell nanofluid with Arrhenius activation energy and gyrotactic motile microorganisms. *Heliyon*, 10(3).
- [10] Waini, I., Ishak, A. and Pop, I., 2024. Eyring-Powell Fluid Flow Past a Shrinking Sheet: Effect of Magnetohydrodynamic (MHD) and Joule Heating. *Journal of Advanced Research in Fluid Mechanics and Thermal Sciences*, 116(1), pp.64-77.
- [11] Riaz, N., 2019. *Thermal Radiation Effect on an MHD Eyring-Powell Fluid Flow* (Doctoral dissertation, CAPITAL UNIVERSITY).
- [12] Ziegenhagen, A., 1965. The very slow flow of a Powell-Eyring fluid around a sphere. *Applied Scientific Research, Section A*, 14(1), pp.43-56.

- [13] Sirohi, V., Timol, M.G. and Kalthia, N.L., 1987. Powell-Eyring model flow near an accelerated plate. *Fluid dynamics research*, 2(3), p.193.
- [14] Yoon, H.K. and Ghajar, A.J., 1987. A note on the Powell-Eyring fluid model. *International communications in heat and mass transfer*, 14(4), pp.381-390.
- [15] Malik, M.Y., Hussain, A. and Nadeem, S., 2013. Boundary layer flow of an Eyring–Powell model fluid due to a stretching cylinder with variable viscosity. *Scientia Iranica*, 20(2), pp.313-321.
- [16] Malik, M.Y., Hussain, A. and Nadeem, S., 2013. Boundary layer flow of an Eyring–Powell model fluid due to a stretching cylinder with variable viscosity. *Scientia Iranica*, 20(2), pp.313-321.
- [17] Akbar, N.S., Ebaid, A. and Khan, Z.H., 2015. Numerical analysis of magnetic field effects on Eyring-Powell fluid flow towards a stretching sheet. *Journal of magnetism and Magnetic Materials*, 382, pp.355-358.
- [18] Kumar, B. and Srinivas, S., 2020. Unsteady hydromagnetic flow of Eyring-Powell nanofluid over an inclined permeable stretching sheet with joule heating and thermal radiation. *Journal of Applied and Computational Mechanics*, 6(2), pp.259-270.
- [19] Pal, D. and Mondal, S.K., 2019. Magneto-bioconvection of Powell Eyring nanofluid over a permeable vertical stretching sheet due to gyrotactic microorganisms in the presence of nonlinear thermal radiation and Joule heating. *International Journal of Ambient Energy*, pp.1-12.
- [20] Hassan, M., Ahsan, M., Usman, Alghamdi, M. and Muhammad, T., 2023. Entropy generation and flow characteristics of Powell Eyring fluid under effects of time scale and viscosities parameters. *Scientific Reports*, 13(1), p.8376.
- [21] Patil, P.M. and Benawadi, S., 2023. The bioconvective flow of an Eyring-Powell nanoliquid: the influence of entropy. *International Journal of Modelling and Simulation*, pp.1-15.
- [22] Patil, P.M. and Goudar, B., 2023. Impact of impulsive motion on the Eyring-Powell nanofluid flow across a rotating sphere in MHD convective regime: entropy analysis. *Journal of Magnetism and Magnetic Materials*, 571, p.170590.

- [23] Ishaq, M., Ali, G., Shah, Z., Islam, S. and Muhammad, S., 2018. Entropy generation on nanofluid thin film flow of Eyring–Powell fluid with thermal radiation and MHD effect on an unsteady porous stretching sheet. *Entropy*, 20(6), p.412.
- [24] Alsaedi, A., Hayat, T., Qayyum, S. and Yaqoob, R., 2020. Eyring–Powell nanofluid flow with nonlinear mixed convection: entropy generation minimization. *Computer methods and programs in biomedicine*, 186, p.105183.
- [25] Bhatti, M.M., Abbas, T., Rashidi, M.M., Ali, M.E.S. and Yang, Z., 2016. Entropy generation on MHD Eyring–Powell nanofluid through a permeable stretching surface. *Entropy*, 18(6), p.224.
- [26] Nazeer, M., Ahmad, F., Saleem, A., Saeed, M., Naveed, S., Shaheen, M. and Al Aidarous, E., 2019. Effects of constant and space-dependent viscosity on Eyring–Powell fluid in a pipe: Comparison of the perturbation and explicit finite difference methods. *Zeitschrift für Naturforschung A*, 74(11), pp.961-969.
- [27] Mubbashar, N., M Ijaz, K., M Usman, R. and Niaz B, K., Numerical and scale analysis of Eyring-Powell nanofluid towards a magnetized stretched Riga surface with entropy generation and internal resistance. *International Communications in Heat and Mass Transfer*.
- [28] Mushtaq, A., Mustafa, M., Hayat, T., Rahi, M. and Alsaedi, A., 2013. Exponentially stretching sheet in a Powell–Eyring fluid: numerical and series solutions. *Zeitschrift für Naturforschung A*, 68(12), pp.791-798.
- [29] Timofeeva, E.V., Routbort, J.L. and Singh, D., 2009. Particle shape effects on thermophysical properties of alumina nanofluids. *Journal of applied physics*, 106(1).
- [30] Anjum, N., Khan, W.A., Hobiny, A., Azam, M., Waqas, M. and Irfan, M., 2022. Numerical analysis for thermal performance of modified Eyring Powell nanofluid flow subject to activation energy and bioconvection dynamic. *Case Studies in Thermal Engineering*, 39, p.102427.
- [31] Iranian, D., Karthik, S. and Seethalakshmy, A., 2023. Heat generation effects on Magnetohydrodynamic Powell-Eyring fluid flow along a vertical surface with a Chemical reaction. *Forces in Mechanics*, 12, p.100212.

- [32] Bariya, H.G. and Patel, M.P., 2024. On the Solution of Blasius Boundary Layer Equations of Prandtl-Eyring Fluid Flow Past a Stretching Sheet. *Indian Journal of Science and Technology*, 17(12), pp.1237-1244.